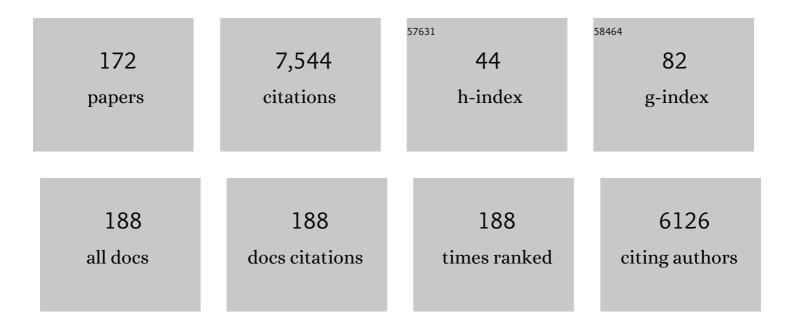
## **Gerhard Glatting**

List of Publications by Year in descending order

Source: https://exaly.com/author-pdf/1396928/publications.pdf Version: 2024-02-01



#	Article	IF	CITATIONS
1	Quantitative analysis of regional distribution of tau pathology with 11C-PBB3-PET in a clinical setting. PLoS ONE, 2022, 17, e0266906.	1.1	7
2	Effect of Tumor Perfusion and Receptor Density on Tumor Control Probability in <sup>177</sup> Lu-DOTATATE Therapy: An In Silico Analysis for Standard and Optimized Treatment. Journal of Nuclear Medicine, 2021, 62, 92-98.	2.8	13
3	Important pharmacokinetic parameters for individualization of <sup>177</sup> Luâ€PSMA therapy: A global sensitivity analysis for a physiologicallyâ€based pharmacokinetic model. Medical Physics, 2021, 48, 556-568.	1.6	10
4	Performance assessment of the ALBIRA II pre-clinical SPECT S102 system for 99mTc imaging. Annals of Nuclear Medicine, 2021, 35, 111-120.	1.2	2
5	A knowledgeâ€based quantitative approach to characterize treatment plan quality: Application to prostate VMAT planning. Medical Physics, 2021, 48, 94-104.	1.6	2
6	Mathematical Modeling of In Vivo Alpha Particle Generators and Chelator Stability. Cancer Biotherapy and Radiopharmaceuticals, 2021, , .	0.7	5
7	Comparison of MRI-based and PET-based image pre-processing for quantification of 11C-PBB3 uptake in human brain. Zeitschrift Fur Medizinische Physik, 2021, 31, 37-47.	0.6	1
8	Changes in Eosinophil as potential marker for immune-related changes associated with PRRT in NET. Nuklearmedizin - NuclearMedicine, 2021, 60, .	0.3	0
9	EANM position paper on the role of radiobiology in nuclear medicine. European Journal of Nuclear Medicine and Molecular Imaging, 2021, 48, 3365-3377.	3.3	23
10	A Whole-Body Physiologically Based Pharmacokinetic Model for Alpha Particle Emitting Bismuth in Rats. Cancer Biotherapy and Radiopharmaceuticals, 2021, , .	0.7	2
11	Comparison of Quantification of Target-Specific Accumulation of [18F]F-siPSMA-14 in the HET-CAM Model and in Mice Using PET/MRI. Cancers, 2021, 13, 4007.	1.7	10
12	An in silico study on the effect of the radionuclide half-life on PET/CT imaging with PSMA-targeting radioligands. Nuklearmedizin - NuclearMedicine, 2021, 60, 33-37.	0.3	1
13	A Physiologically Based Pharmacokinetic Model for In Vivo Alpha Particle Generators Targeting Neuroendocrine Tumors in Mice. Pharmaceutics, 2021, 13, 2132.	2.0	9
14	A population-based method to determine the time-integrated activity in molecular radiotherapy. EJNMMI Physics, 2021, 8, 82.	1.3	10
15	Multi-Modal PET and MR Imaging in the Hen's Egg Test-Chorioallantoic Membrane (HET-CAM) Model for Initial In Vivo Testing of Target-Specific Radioligands. Cancers, 2020, 12, 1248.	1.7	18
16	MITIGATE-NeoBOMB1, a Phase I/IIa Study to Evaluate Safety, Pharmacokinetics, and Preliminary Imaging of <sup>68</sup> Ga-NeoBOMB1, a Gastrin-Releasing Peptide Receptor Antagonist, in GIST Patients. Journal of Nuclear Medicine, 2020, 61, 1749-1755.	2.8	27
17	Influence of sampling schedules on [177Lu]Lu-PSMA dosimetry. EJNMMI Physics, 2020, 7, 41.	1.3	27
18	Modeling sphere dynamics in blood vessels for SIRT pre-planning – To fathom the potential and limitations. Zeitschrift Fur Medizinische Physik, 2019, 29, 5-15.	0.6	1

#	Article	IF	CITATIONS
19	Modeling and Predicting Tumor Response in Radioligand Therapy. Journal of Nuclear Medicine, 2019, 60, 65-70.	2.8	41
20	Modelling the internalisation process of prostate cancer cells for PSMA-specific ligands. Nuclear Medicine and Biology, 2019, 72-73, 20-25.	0.3	6
21	Radiation-induced malignancies after intensity-modulated versus conventional mediastinal radiotherapy in a small animal model. Scientific Reports, 2019, 9, 15489.	1.6	4
22	Technical Note: Optimal sampling schedules for kidney dosimetry based on the hybrid planar/SPECT method in 177 Luâ€PSMA therapy. Medical Physics, 2019, 46, 5861-5866.	1.6	11
23	The effect of ligand amount, affinity and internalization on PSMA-targeted imaging and therapy: A simulation study using a PBPK model. Scientific Reports, 2019, 9, 20041.	1.6	28
24	A simulation-based method to determine optimal sampling schedules for dosimetry in radioligand therapy. Zeitschrift Fur Medizinische Physik, 2019, 29, 314-325.	0.6	10
25	The Effect of Total Tumor Volume on the Biologically Effective Dose to Tumor and Kidneys for <sup>177</sup> Lu-Labeled PSMA Peptides. Journal of Nuclear Medicine, 2018, 59, 929-933.	2.8	54
26	A Method for Point Spread Function Estimation for Accurate Quantitative Imaging. IEEE Transactions on Nuclear Science, 2018, 65, 961-969.	1.2	3
27	[OA142] Validation framework for automated determination of the optimal number of clusters in [F-18]FET-PET brain images. Physica Medica, 2018, 52, 54.	0.4	0
28	EANM practical guidance on uncertainty analysis for molecular radiotherapy absorbed dose calculations. European Journal of Nuclear Medicine and Molecular Imaging, 2018, 45, 2456-2474.	3.3	124
29	Treatment planning algorithm for peptide receptor radionuclide therapy considering multiple tumor lesions and organs at risk. Medical Physics, 2018, 45, 3516-3523.	1.6	15
30	Radiation Dosimetry in Ibritumomab Therapy. Resistance To Targeted Anti-cancer Therapeutics, 2018, , 105-117.	0.1	0
31	Combined stereotactic biopsy and stepping-source interstitial irradiation of glioblastoma multiforme. Journal of Neurosurgical Sciences, 2018, 62, 214-220.	0.3	2
32	Collimator optimization for small animal radiation therapy at a micro-CT. Zeitschrift Fur Medizinische Physik, 2017, 27, 56-64.	0.6	2
33	Comparison of five cluster validity indices performance in brain [ <sup>18</sup> F] <scp>FET</scp> â€ <scp>PET</scp> image segmentation using <i>k</i> â€means. Medical Physics, 2017, 44, 209-220.	1.6	13
34	Investigation of the imaging characteristics of the ALBIRA II small animal PET system for 18 F, 68 Ga and 64 Cu. Zeitschrift Fur Medizinische Physik, 2017, 27, 132-144.	0.6	9
35	Focus on the Low-Dose Bath: No Increased Cancer Risk After Mediastinal VMAT Versus AP/PA Irradiation in a Tumor-Prone Rat Model. International Journal of Radiation Oncology Biology Physics, 2017, 99, S76-S77.	0.4	2
36	Prediction of time-integrated activity coefficients in PRRT using simulated dynamic PET and a pharmacokinetic model. Physica Medica, 2017, 42, 298-304.	0.4	15

#	Article	IF	CITATIONS
37	Treatment planning in PRRT based on simulated PET data and a PBPK model. Nuklearmedizin - NuclearMedicine, 2017, 56, 23-30.	0.3	11
38	Session 2. Cells, materials and biochemistry I. Biomedizinische Technik, 2017, 62, .	0.9	0
39	Physikalisch-technische Grundlagen und Tracerentwicklung in der Positronenemissionstomografie. , 2017, , 19-56.		0
40	A single-source photon source model of a linear accelerator for Monte Carlo dose calculation. PLoS ONE, 2017, 12, e0183486.	1.1	3
41	<sup>19</sup> F Oximetry with semifluorinated alkanes. Artificial Cells, Nanomedicine and Biotechnology, 2016, 44, 1861-1866.	1.9	7
42	Timeâ€integrated activity coefficient estimation for radionuclide therapy using PET and a pharmacokinetic model: A simulation study on the effect of sampling schedule and noise. Medical Physics, 2016, 43, 5145-5154.	1.6	18
43	Sensitivity Analysis of a Physiologically Based Pharmacokinetic Model Used for Treatment Planning in Peptide Receptor Radionuclide Therapy. Cancer Biotherapy and Radiopharmaceuticals, 2016, 31, 217-224.	0.7	8
44	Cumulative radiation exposure from imaging procedures and associated lifetime cancer risk for patients with lymphoma. Scientific Reports, 2016, 6, 35181.	1.6	38
45	Comparison of breast sequential and simultaneous integrated boost using the biologically effective dose volume histogram (BEDVH). Radiation Oncology, 2016, 11, 16.	1.2	14
46	Dependence of treatment planning accuracy in peptide receptor radionuclide therapy on the sampling schedule. EJNMMI Research, 2016, 6, 30.	1.1	29
47	Optimized Peptide Amount and Activity for <sup>90</sup> Y-Labeled DOTATATE Therapy. Journal of Nuclear Medicine, 2016, 57, 503-508.	2.8	45
48	Physiologically based pharmacokinetic modeling of 18F-SiFAlin-Asp3-PEG1-TATE in AR42J tumor bearing mice. Nuclear Medicine and Biology, 2016, 43, 243-246.	0.3	2
49	The role of patient-based treatment planning in peptide receptor radionuclide therapy. European Journal of Nuclear Medicine and Molecular Imaging, 2016, 43, 871-880.	3.3	47
50	Investigating the Effect of Ligand Amount and Injected Therapeutic Activity: A Simulation Study for 177Lu-Labeled PSMA-Targeting Peptides. PLoS ONE, 2016, 11, e0162303.	1.1	30
51	Imaging of Orthotopic Glioblastoma Xenografts in Mice Using a Clinical CT Scanner: Comparison with Micro-CT and Histology. PLoS ONE, 2016, 11, e0165994.	1.1	17
52	The HIV-derived protein Vpr52-96 has anti-glioma activity in vitro and in vivo. Oncotarget, 2016, 7, 45500-45512.	0.8	1
53	Comparison of breast simultaneous integrated boost (SIB) radiotherapy techniques. Radiation Oncology, 2015, 10, 139.	1.2	34
54	Image-Guided Radiotherapy Using a Modified Industrial Micro-CT for Preclinical Applications. PLoS ONE, 2015, 10, e0126246.	1.1	19

#	Article	IF	CITATIONS
55	Physiologically Based Pharmacokinetic Modeling Is Essential in 90Y-Labeled Anti-CD66 Radioimmunotherapy. PLoS ONE, 2015, 10, e0127934.	1.1	20
56	Population-Based Modeling Improves Treatment Planning Before 90Y-Labeled Anti-CD66 Antibody Radioimmunotherapy. Cancer Biotherapy and Radiopharmaceuticals, 2015, 30, 285-290.	0.7	6
57	In vivo micro-CT imaging of untreated and irradiated orthotopic glioblastoma xenografts in mice: capabilities, limitations and a comparison with bioluminescence imaging. Journal of Neuro-Oncology, 2015, 122, 245-254.	1.4	19
58	Technical prerequisites and imaging protocols for CT perfusion imaging in oncology. European Journal of Radiology, 2015, 84, 2359-2367.	1.2	31
59	A multicentre comparison of quantitative 90Y PET/CT for dosimetric purposes after radioembolization with resin microspheres. European Journal of Nuclear Medicine and Molecular Imaging, 2015, 42, 1202-1222.	3.3	131
60	Knowledge-based radiation therapy (KBRT) treatment planning versus planning by experts: validation of a KBRT algorithm for prostate cancer treatment planning. Radiation Oncology, 2015, 10, 111.	1.2	67
61	The NUKDOS software for treatment planning in molecular radiotherapy. Zeitschrift Fur Medizinische Physik, 2015, 25, 264-274.	0.6	41
62	Comparison of Knowledge Based Radiation Therapy Treatment Plans Against Expert Plans for Prostate VMAT. International Journal of Radiation Oncology Biology Physics, 2015, 93, E582.	0.4	0
63	Comparison of Breast Sequential and Simultaneous Integrated Boost Using the Biologically Effective Dose Volume Histogram (BEDVH). International Journal of Radiation Oncology Biology Physics, 2015, 93, E14-E15.	0.4	0
64	The HIV-Derived Protein Vpr52-96 Has Antiglioma Activity In Vitro and In Vivo. International Journal of Radiation Oncology Biology Physics, 2015, 93, S141-S142.	0.4	0
65	Abstract 4458: The HIV-derived protein Vpr52-96has anti-glioma activity in vitro and in vivo. , 2015, , .		Ο
66	Quantitative and Qualitative Assessment of Yttrium-90 PET/CT Imaging. PLoS ONE, 2014, 9, e110401.	1.1	44
67	Second cancer risk after 3D-CRT, IMRT and VMAT for breast cancer. Radiotherapy and Oncology, 2014, 110, 471-476.	0.3	138
68	Converting a Standard Micro-CT Into an IGRT-Competent Small Animal Irradiation Device. International Journal of Radiation Oncology Biology Physics, 2014, 90, S804-S805.	0.4	1
69	Breast Radiation Therapy (RT) Using Simultaneous Integrated Boost (SIB): Which Is the Optimal Intensity Modulated RT (IMRT) Technique?. International Journal of Radiation Oncology Biology Physics, 2014, 90, S227-S228.	0.4	Ο
70	Arc therapy for total body irradiation – A robust novel treatment technique for standard treatment rooms. Radiotherapy and Oncology, 2014, 110, 553-557.	0.3	34
71	Intraoperative radiation therapy. Zeitschrift Fur Medizinische Physik, 2014, 24, 1-2.	0.6	0
72	Dependence of image quality on acquisition time for the PET/CT Biograph mCT. Zeitschrift Fur Medizinische Physik, 2014, 24, 73-79.	0.6	14

#	Article	IF	CITATIONS
73	A fast method for rescaling voxel S values for arbitrary voxel sizes in targeted radionuclide therapy from a single Monte Carlo calculation. Medical Physics, 2013, 40, 082502.	1.6	15
74	Treatment planning in molecular radiotherapy. Zeitschrift Fur Medizinische Physik, 2013, 23, 262-269.	0.6	44
75	Molecular radiotherapy: The NUKFIT software for calculating the timeâ€integrated activity coefficient. Medical Physics, 2013, 40, 102504.	1.6	73
76	Differences in predicted and actually absorbed doses in peptide receptor radionuclide therapy. Medical Physics, 2012, 39, 5708-5717.	1.6	42
77	A Monte Carlo based source model for dose calculation of endovaginal TARGIT brachytherapy with INTRABEAM and a cylindrical applicator. Zeitschrift Fur Medizinische Physik, 2012, 22, 197-204.	0.6	25
78	Auger electron emitter against multiple myeloma — targeted endo-radio-therapy with 1251-labeled thymidine analogue 5-iodo-4′-thio-2′-deoxyuridine. Nuclear Medicine and Biology, 2011, 38, 1067-1077.	0.3	10
79	Radioimmunotherapy-based conditioning for hematopoietic cell transplantation in children with malignant and nonmalignant diseases. Blood, 2011, 117, 4642-4650.	0.6	46
80	Optimal preloading in radioimmunotherapy with anti-CD45 antibody. Medical Physics, 2011, 38, 2572-2578.	1.6	19
81	Dependence of the anti-CD66 antibody biodistribution on the dissociation constant: A simulation study. Zeitschrift Fur Medizinische Physik, 2011, 21, 301-304.	0.6	7
82	Determination of individual organ masses for 90Y-anti-CD66 radioimmunotherapy: Influence on therapy planning. Zeitschrift Fur Medizinische Physik, 2011, 21, 305-309.	0.6	5
83	Nuclear medicine dosimetry: Quantitative imaging and dose calculations. Zeitschrift Fur Medizinische Physik, 2011, 21, 246-247.	0.6	19
84	New Molecular Markers for Prostate Tumor Imaging: A Study on 2â€Methylene Substituted Fatty Acids as New AMACR Inhibitors. Chemistry - A European Journal, 2011, 17, 10144-10150.	1.7	19
85	Analysing saturable antibody binding based on serum data and pharmacokinetic modelling. Physics in Medicine and Biology, 2011, 56, 73-86.	1.6	7
86	Radioimmunotherapy with Anti-CD66 Antibody: Improving the Biodistribution Using a Physiologically Based Pharmacokinetic Model. Journal of Nuclear Medicine, 2010, 51, 484-491.	2.8	42
87	Clinical value of 18F-fluorodihydroxyphenylalanine positron emission tomography/computed tomography (18F-DOPA PET/CT) for detecting pheochromocytoma. European Journal of Nuclear Medicine and Molecular Imaging, 2010, 37, 484-493.	3.3	62
88	EANM Dosimetry Committee guidelines for bone marrow and whole-body dosimetry. European Journal of Nuclear Medicine and Molecular Imaging, 2010, 37, 1238-1250.	3.3	217
89	Potential of Optimal Preloading in Anti-CD20 Antibody Radioimmunotherapy: An Investigation Based on Pharmacokinetic Modeling. Cancer Biotherapy and Radiopharmaceuticals, 2010, 25, 279-287.	0.7	16
90	Clinical Value of 18-Fluorine-Fluorodihydroxyphenylalanine Positron Emission Tomography/Computed Tomography in the Follow-Up of Medullary Thyroid Carcinoma. Thyroid, 2010, 20, 527-533.	2.4	78

#	Article	IF	CITATIONS
91	Cost-Effectiveness of Hybrid PET/CT for Staging of Non–Small Cell Lung Cancer. Journal of Nuclear Medicine, 2010, 51, 1668-1675.	2.8	62
92	Modelling radioimmunotherapy with anti-CD45 antibody to obtain a more favourable biodistribution. Nuklearmedizin - NuclearMedicine, 2009, 48, 113-119.	0.3	6
93	Improving Anti-CD45 Antibody Radioimmunotherapy Using a Physiologically Based Pharmacokinetic Model. Journal of Nuclear Medicine, 2009, 50, 296-302.	2.8	36
94	Comparing time activity curves using the Akaike information criterion. Physics in Medicine and Biology, 2009, 54, N501-N507.	1.6	22
95	Model selection for time-activity curves: The corrected Akaike information criterion and the F-test. Zeitschrift Fur Medizinische Physik, 2009, 19, 200-206.	0.6	94
96	Towards to hENT1-nucleoside transporter selective imaging agents. Synthesis and in vitro evaluation of the radiolabeled SAENTA analogues. Bioorganic and Medicinal Chemistry Letters, 2009, 19, 5151-5154.	1.0	1
97	Performance of Integrated FDG-PET/CT for Differentiating Benign and Malignant Lung Lesions -Results from a Large Prospective Clinical Trial. Molecular Imaging and Biology, 2008, 10, 121-128.	1.3	13
98	[11C]choline PET/CT imaging in occult local relapse of prostate cancer after radical prostatectomy. European Journal of Nuclear Medicine and Molecular Imaging, 2008, 35, 9-17.	3.3	168
99	First Demonstration of Leukemia Imaging with the Proliferation Marker <sup>18</sup> F-Fluorodeoxythymidine. Journal of Nuclear Medicine, 2008, 49, 1756-1762.	2.8	68
100	<i>Short Communication:</i> <sup>18</sup> F-Immuno-PET: Determination of Anti-CD66 Biodistribution in a Patient with High-Risk Leukemia. Cancer Biotherapy and Radiopharmaceuticals, 2008, 23, 819-824.	0.7	14
101	Imaging Bone and Soft Tissue Tumors with the Proliferation Marker [18F]Fluorodeoxythymidine. Clinical Cancer Research, 2008, 14, 2970-2977.	3.2	69
102	Preferential Tumor Targeting and Selective Tumor Cell Cytotoxicity of 5-[131/1251]Iodo-4′-Thio-2′-Deoxyuridine. Clinical Cancer Research, 2008, 14, 7311-7319.	3.2	17
103	Multiple Myeloma: Molecular Imaging with C-Methionine PET/CT—Initial Experience. Radiology, 2007, 242, 498-508.	3.6	105
104	Choosing the optimal fit function: Comparison of the Akaike information criterion and the Fâ€ŧest. Medical Physics, 2007, 34, 4285-4292.	1.6	193
105	Breaking Chemoresistance and Radioresistance with [213Bi]anti-CD45 Antibodies in Leukemia Cells. Cancer Research, 2007, 67, 1950-1958.	0.4	93
106	1231-ITdU-Mediated Nanoirradiation of DNA Efficiently Induces Cell Kill in HL60 Leukemia Cells and in Doxorubicin-, Â-, or Â-Radiation-Resistant Cell Lines. Journal of Nuclear Medicine, 2007, 48, 1000-1007.	2.8	25
107	Direct comparison of [18F]FDG PET/CT with PET alone and with side-by-side PET and CT in patients with malignant melanoma. European Journal of Nuclear Medicine and Molecular Imaging, 2007, 34, 1355-1364.	3.3	53
108	Early assessment of therapy response in malignant lymphoma with the thymidine analogue [18F]FLT. European Journal of Nuclear Medicine and Molecular Imaging, 2007, 34, 1775-1782.	3.3	62

#	Article	IF	CITATIONS
109	Radiosynthesis and evaluation of [11C]BTA-1 and [11C]3'-Me-BTA-1 as potential radiotracers for in vivo imaging of-amyloid plaques. Nuklearmedizin - NuclearMedicine, 2007, , .	0.3	1
110	Radioimmunotherapy for Myeloablation Before SCT in Paediatric Patients with Malignant and Non-Malignant Diseases Blood, 2007, 110, 624-624.	0.6	17
111	Determination of the Immunoreactivity of Radiolabeled Monoclonal Antibodies: A Theoretical Analysis. Cancer Biotherapy and Radiopharmaceuticals, 2006, 21, 15-21.	0.7	4
112	Molecular Imaging of Proliferation in Malignant Lymphoma. Cancer Research, 2006, 66, 11055-11061.	0.4	173
113	Bone marrow transplantation nephropathy after an intensified conditioning regimen with radioimmunotherapy and allogeneic stem cell transplantation. Journal of Nuclear Medicine, 2006, 47, 278-86.	2.8	16
114	Targeted marrow irradiation with radioactively labeled anti-CD66 monoclonal antibody prior to allogeneic stem cell transplantation for patients with leukemia: results of a phase I-II study. Haematologica, 2006, 91, 285-6.	1.7	15
115	Imaging prostate cancer with 11C-choline PET/CT. Journal of Nuclear Medicine, 2006, 47, 1249-54.	2.8	191
116	Anti-CD45 monoclonal antibody YAML568: A promising radioimmunoconjugate for targeted therapy of acute leukemia. Journal of Nuclear Medicine, 2006, 47, 1335-41.	2.8	27
117	188Re or 90Y-labelled anti-CD66 antibody as part of a dose-reduced conditioning regimen for patients with acute leukaemia or myelodysplastic syndrome over the age of 55: results of a phase I-II study. British Journal of Haematology, 2005, 130, 604-613.	1.2	92
118	Clinical relevance of imaging proliferative activity in lung nodules. European Journal of Nuclear Medicine and Molecular Imaging, 2005, 32, 525-533.	3.3	101
119	Internal radionuclide therapy: The ULMDOS software for treatment planning. Medical Physics, 2005, 32, 2399-2405.	1.6	36
120	Radiation exposure of patients undergoing whole-body dual-modality 18F-FDG PET/CT examinations. Journal of Nuclear Medicine, 2005, 46, 608-13.	2.8	298
121	Lymph Node Staging in Lung Cancer Using [18F]FDG-PET. Thoracic and Cardiovascular Surgeon, 2004, 52, 96-101.	0.4	35
122	Improving binding potential analysis in [11C]raclopride PET studies using cluster analysis. Medical Physics, 2004, 31, 902-906.	1.6	6
123	Quantitative Imaging Of Yttrium-86 Pet with the Ecat Exact Hr+ In 2D Mode. Cancer Biotherapy and Radiopharmaceuticals, 2004, 19, 482-490.	0.7	20
124	[ 18 F] 3-deoxy-3′-fluorothymidine positron emission tomography: alternative or diagnostic adjunct to 2-[ 18 f]-fluoro-2-deoxy- d -glucose positron emission tomography in the workup of suspicious central focal lesions?. Journal of Thoracic and Cardiovascular Surgery, 2004, 127, 1093-1099.	0.4	33
125	Omission of bone scanning according to staging guidelines leads to futile therapy in non-small cell lung cancer. European Journal of Nuclear Medicine and Molecular Imaging, 2004, 31, 964-8.	3.3	46
126	Imaging of activated microglia with PET and [11 C]PK 11195 in corticobasal degeneration. Movement Disorders, 2004, 19, 817-821.	2.2	39

#	Article	IF	CITATIONS
127	Quantitative Imaging of Yttrium-86 PET with the ECAT EXACT HR <sup>+</sup> in 2D Mode. Cancer Biotherapy and Radiopharmaceuticals, 2004, 19, 482-490.	0.7	4
128	Quantification of 18F-FDG uptake in non-small cell lung cancer: a feasible prognostic marker?. Journal of Nuclear Medicine, 2004, 45, 1274-6.	2.8	8
129	F-18 NaF PET for Detection of Bone Metastases in Lung Cancer: Accuracy, Cost-Effectiveness, and Impact on Patient Management. Journal of Bone and Mineral Research, 2003, 18, 2206-2214.	3.1	155
130	A comparison of the biodistribution and biokinetics of 99mTc-anti-CD66 mAb BW 250/183 and 99mTc-anti-CD45 mAb YTH 24.5 with regard to suitability for myeloablative radioimmunotherapy. European Journal of Nuclear Medicine and Molecular Imaging, 2003, 30, 667-673.	3.3	22
131	[18F]5-Fluoro-2-Deoxyuridine-PET for Imaging of Malignant Tumors and for Measuring Tissue Proliferation. Cancer Biotherapy and Radiopharmaceuticals, 2003, 18, 327-337.	0.7	15
132	ROC analysis for assessment of lesion detection performance in 3D PET: Influence of reconstruction algorithms. Medical Physics, 2003, 30, 2315-2319.	1.6	8
133	Quantitative image reconstruction in PET from emission data only using cluster analysis. Zeitschrift Fur Medizinische Physik, 2003, 13, 269-274.	0.6	3
134	Imaging proliferation in lung tumors with PET: 18F-FLT versus 18F-FDG. Journal of Nuclear Medicine, 2003, 44, 1426-31.	2.8	281
135	Simultaneous iterative reconstruction of emission and attenuation images in positron emission tomography from emission data only. Medical Physics, 2002, 29, 1962-1967.	1.6	20
136	Myeloablative Radioimmunotherapy with Re-188-anti-CD66-Antibody for Conditioning of High-Risk Leukemia Patients Prior to Stem Cell Transplantation: Biodistribution, Biokinetics and Immediate Toxicities. Cancer Biotherapy and Radiopharmaceuticals, 2002, 17, 151-163.	0.7	38
137	Evaluation of pyrimidine metabolising enzymes and in vitro uptake of 3'-[18F]fluoro-3'-deoxythymidine ([18F]FLT) in pancreatic cancer cell lines. European Journal of Nuclear Medicine and Molecular Imaging, 2002, 29, 1174-1181.	3.3	70
138	A survey of PET activity in Germany during 1999. European Journal of Nuclear Medicine and Molecular Imaging, 2002, 29, 1091-1097.	3.3	20
139	FDG uptake in breast cancer: correlation with biological and clinical prognostic parameters. European Journal of Nuclear Medicine and Molecular Imaging, 2002, 29, 1317-1323.	3.3	274
140	3-deoxy-3-[(18)F]fluorothymidine-positron emission tomography for noninvasive assessment of proliferation in pulmonary nodules. Cancer Research, 2002, 62, 3331-4.	0.4	162
141	Targeted bone marrow irradiation in the conditioning of high-risk leukaemia prior to stem cell transplantation. European Journal of Nuclear Medicine and Molecular Imaging, 2001, 28, 807-815.	2.2	36
142	Validation of myocardial blood flow estimation with nitrogen-13 ammonia PET by the argon inert gas technique in humans. European Journal of Nuclear Medicine and Molecular Imaging, 2001, 28, 340-345.	2.2	13
143	Fluorine-18 2-deoxy-2-fluoro-D-glucose PET in the preoperative staging of breast cancer: comparison with the standard staging procedures. European Journal of Nuclear Medicine and Molecular Imaging, 2001, 28, 351-358.	2.2	225
144	Rhenium 188–labeled anti-CD66 (a, b, c, e) monoclonal antibody to intensify the conditioning regimen prior to stem cell transplantation for patients with high-risk acute myeloid leukemia or myelodysplastic syndrome: results of a phase I-II study. Blood, 2001, 98, 565-572.	0.6	166

#	Article	IF	CITATIONS
145	2-(fluorine-18)fluoro-2-deoxy-D-glucose positron emission tomography in the detection and staging of malignant lymphoma. Cancer, 2001, 91, 889-899.	2.0	221
146	2â€(fluorineâ€18)fluoroâ€2â€deoxyâ€Dâ€glucose positron emission tomography in the detection and staging of malignant lymphoma. Cancer, 2001, 91, 889-899.	2.0	2
147	Dynamical Cluster Analysis for the Detection of Microglia Activation. , 2001, , 442-445.		1
148	Values and Limitations of 18F-Fluorodeoxyglucose???Positron-Emission Tomography with Preoperative Evaluation of Patients with Pancreatic Masses. Pancreas, 2000, 20, 109-116.	0.5	151
149	In vivo imaging of activated microglia using [11 C]PK11195 and positron emission tomography in patients after ischemic stroke. NeuroReport, 2000, 11, 2957-2960.	0.6	121
150	Simultaneous iterative reconstruction for emission and attenuation images in positron emission tomography. Medical Physics, 2000, 27, 2065-2071.	1.6	20
151	Early Detection and Accurate Description of Extent of Metastatic Bone Disease in Breast Cancer With Fluoride Ion and Positron Emission Tomography. Journal of Clinical Oncology, 1999, 17, 2381-2381.	0.8	266
152	lterative reconstruction for attenuation correction in positron emission tomography: Maximum likelihood for transmission and blank scan. Medical Physics, 1999, 26, 1838-1842.	1.6	5
153	Treatment of radioactive decay in pharmacokinetic modeling: Influence on parameter estimation in cardiac 13N-PET. Medical Physics, 1999, 26, 616-621.	1.6	17
154	Preparation and evaluation of the rhenium-188-labelled anti-NCA antigen monoclonal antibody BW 250/183 for radioimmunotherapy of leukaemia. European Journal of Nuclear Medicine and Molecular Imaging, 1999, 26, 1265-1273.	3.3	48
155	F-18 Fluorodeoxyglucose (FDC) and C-Reactive Protein (CRP). Molecular Imaging and Biology, 1999, 2, 131-136.	0.3	18
156	Chronic osteomyelitis: detection with FDG PET and correlation with histopathologic findings Radiology, 1998, 206, 749-754.	3.6	200
157	Iterative image reconstruction reduces apparent tumor distortion Radiology, 1997, 204, 279-279.	3.6	12
158	Functionality dependence for molecular nonaffine deformation of polymer networks. Polymer, 1997, 38, 4049-4052.	1.8	3
159	Blurring of Vessels in Spiral CT Angiography: Effects of Collimation Width, Pitch, Viewing Plane, and Windowing in Maximum Intensity Projection. Journal of Computer Assisted Tomography, 1996, 20, 965-974.	0.5	32
160	Freely jointed chain with variable segment number and length. Colloid and Polymer Science, 1995, 273, 32-37.	1.0	8
161	Polymer chains with correlations between adjacent segments: Qualitative differences to the freely jointed chain. Journal of Chemical Physics, 1995, 102, 3448-3451.	1.2	1
162	2-(fluorine-18)-fluoro-2-deoxy-D-glucose PET in detection of pancreatic cancer: value of quantitative image interpretation Radiology, 1995, 195, 339-344.	3.6	149

#	Article	IF	CITATIONS
163	Microscopic Nonaffine Deformation of Polydisperse Polymer Networks. Macromolecules, 1995, 28, 5906-5909.	2.2	9
164	Analytical model for the microscopic nonaffine deformation of polymer networks. Journal of Chemical Physics, 1994, 101, 2532-2538.	1.2	18
165	Are the continuum and the lattice representation of freely jointed chains equivalent?. Macromolecular Theory and Simulations, 1994, 3, 575-583.	0.6	7
166	Pathophysiological Basis and Clinical Value of <sup>18</sup> F-Fluorodeoxyglucose and Positron Emission Tomography in Pancreatic Adenocarcinoma. Digestive Surgery, 1994, 11, 360-365.	0.6	3
167	Influence of microscopic nonâ€affinity and functionality on the deformation of polymeric networks. Macromolecular Symposia, 1994, 81, 129-137.	0.4	1
168	Partition function and force extension relation for a generalized freely jointed chain. Macromolecules, 1993, 26, 6085-6091.	2.2	32
169	Chaotic Motion of Molecular Chains. NATO ASI Series Series B: Physics, 1991, , 195-214.	0.2	0
170	Effect of vasoactive intestinal polypeptide (VIP) on glucose and lipid metabolism of isolated rat adipocytes. Research in Experimental Medicine, 1988, 188, 189-195.	0.7	5
171	Endogenous Opiates Do Not Influence Glucose and Lipid Metabolism in Rat Adipocytes. Experimental and Clinical Endocrinology and Diabetes, 1988, 91, 350-354.	0.6	8
172	Effects of Gastric Inhibitory Polypeptide on Glucose and Lipid Metabolism of Isolated Rat Adipocytes. Annals of Nutrition and Metabolism, 1988, 32, 282-288.	1.0	75